Iranian Journal of Materials Forming 11 (3) (2024) 50-65

Online ISSN: 2383-0042

IJMF

Iranian Journal of Materials Forming

Journal Homepage: http://ijmf.shirazu.ac.ir

Research Article

Fabrication and Evaluation of Diopside/Gelatin Composite Scaffolds for Bone Tissue Engineering: A Comprehensive Study on Porosity, Bioactivity and Cell Interactions

H. Ghomi[1*] and A. Shams[1, 2]

[1] Advanced Materials Research Center, Department of Materials Engineering, Najafabad Branch, Islamic Azad University, Najafabad, Iran
[2] Department of Stem Cells and Regenerative Medicine, Institute for Medical Biotechnology, National Institute of Genetic Engineering and Biotechnology (NIGEB), Tehran, Iran

ARTICLE INFO

Article history:

Received 27 September 2024
Reviewed 23 November 2024
Revised 17 December 2024
Accepted 27 December 2024

Keywords:

Bone scaffold
Tissue engineering
Diopside scaffold
Gelatin coating

Please cite this article as:

Ghomi, H., & Shams, A. (2024). Fabrication and evaluation of diopside/gelatin composite scaffolds for bone tissue engineering: A comprehensive study on porosity, bioactivity and cell interactions. *Iranian Journal of Materials Forming*, *11*(3), 50-65. https://doi.org/10.22099/IJMF.2025.51294.1304

ABSTRACT

This research investigates the development and characterization of a novel diopside/gelatin composite scaffold tailored to enhance bone tissue regeneration. The scaffold was fabricated using a space holder method followed by a gelatin coating technique. Energy-dispersive X-ray spectroscopy (EDS) analysis confirmed the successful application of the gelatin coating on the diopside scaffold. Scanning electron microscopy (SEM) revealed a highly porous, interconnected architecture, which provides an optimal environment for cell infiltration, vascularization, and nutrient diffusion, thereby promoting bone ingrowth. Mechanical testing demonstrated that the composite scaffolds exhibit sufficient compressive strength and stiffness to withstand physiological loads, supporting new bone tissue formation. Biological evaluation revealed excellent biocompatibility, with the scaffolds supporting robust cell attachment and proliferation. Furthermore, the observed elevation in alkaline phosphatase (ALP) activity, a critical marker of osteogenic differentiation, highlights the scaffolds' osteoconductive potential and their ability to facilitate bone formation. The synergistic combination of diopside, a bioactive ceramic renowned for its biocompatibility and osteoconductive properties, and gelatin, a natural biopolymer providing a cell-friendly environment and enhancing cell adhesion, has resulted in a promising composite scaffold significantly improved for bone tissue engineering. Notably, the application of a gelatin coating on the diopside scaffold significantly improved cell interaction and attachment, improving the overall bioactivity of the construct. These findings underscore the potential of the diopside/gelatin composite scaffold for bone regeneration applications. Nevertheless, further in vivo investigation and clinical studies are necessary to fully validate the scaffold's efficacy and elucidate its potential for clinical studies.

1. Introduction

Scaffolds for bone tissue engineering have emerged as a promising alternative to synthetic implants for repairing damaged bones. Successful bone tissue repair and tissue engineering require bioactive materials with appropriate mechanical properties and biodegradability [1-3].

* Corresponding author
E-mail address: hamed1985.gh@gmail.com (H. Ghomi)
https://doi.org/10.22099/IJMF.2025.51294.1304

Ceramics are widely used in repairing bone tissue due to their favorable properties. Among them, ceramic-based calcium silicates have excellent bioactivity, making them a prominent focus in bone tissue engineering applications. Examples include wollastonite (low-temperature, triclinic $CaSiO_3$), pseudo-wollastonite (high-temperature, monoclinic $CaSiO_3$), akermanite ($Ca_2MgSi_2O_7$), and diopside ($CaMgSi_2O_6$). Diopside, a ceramic containing silicon (Si), calcium (Ca), and magnesium (Mg), is particularly notable for its slower degradation rate and its ability to form apatite in vitro study [4-6].

Extensive research has demonstrated the potential of diopside powder as a suitable material for bone tissue regeneration. While diopside shares a similar chemical composition to $CaSiO_3$ and akermanite, its slower degradation rate enhances its suitability for bone tissue engineering, which allows for proper integration with surrounding tissue and a gradual replacement by natural bone [7-9].

Diopside, a member of the CaO-MgO-SiO_2 ternary system, is known for its high mechanical strength and excellent biocompatibility. These properties make it a promising material for bone tissue engineering. Recent studies have shown that diopside-based scaffolds not only possess desirable mechanical properties but also effectively support cell growth and tissue regeneration. This further emphasizes the potential of diopside in the field of bone tissue engineering [10-12].

Due to the limitations of ceramics in terms of mechanical properties, ceramic-polymer composite scaffolds have emerged as a superior option for bone tissue engineering. Several studies have demonstrated the improved mechanical properties of composite scaffolds compared to other types. However, their use may still be limited in certain situations, particularly due to their low fracture toughness [13-15].

In recent years, there has been a growing trend toward using polymer coatings on ceramic scaffolds, primarily due to their potential for mechanical enhancement. The combination of ceramics and polymers in a scaffold provides both strength and toughness, which are essential for bone tissue engineering. The improved strength of the coated structure can be attributed to the mechanism of defect formation, as the polymer coating effectively fills in microporosities and microcracks, making it more difficult for them to propagate. Additionally, the presence of polymeric fibers in the scaffold acts as an intermediate between the walls of a crack, helping to prevent crack propagation and increase toughness [16-18].

Among the biomaterials used for coating, natural biopolymers stand out as the most suitable option due to their biological origin. They offer excellent biocompatibility, enhanced cell interaction, and superior hydrophilicity compared to synthetic polymers [19-22].

The primary aim of this study was to develop diopside/gelatin composite scaffolds using the space holder technique. These scaffolds were subsequently coated with varying concentrations of gelatin solution. Their porosity, pore morphology, pore interconnection, bioactivity, cytotoxicity, proliferation, adhesion, and alkaline phosphatase activity were systematically evaluated. The novelty of this study lies in the development of diopside and gelatin within composite scaffolds, utilizing the space holder technique and subsequent gelatin coating. This approach combines the biocompatibility and bioactivity of ceramic-based diopside alongside the enhanced cell interaction and attachment properties of gelatin. By thoroughly examining the scaffolds' properties, including porosity, pore morphology, pore interconnection, bioactivity, cytotoxicity, proliferation, adhesion, and alkaline phosphatase activity, this research provides valuable insights into optimizing composite scaffold design for bone tissue engineering.

2. Experimental Procedure

In this study, tetraethyl orthosilicate (TEOS) (Merk, Germany), magnesium chloride hexahydrate, magnesium nitrate hexahydrate (Sigma Aldrich, USA), calcium nitrate (Sigma Aldrich, USA), and pure ethanol (Sigma Aldrich, USA) were used to prepare diopside powder [23].

2.1. Preparation of diopside powder

Diopside powders were fabricated using the sol-gel method. The raw materials used included calcium nitrate tetrahydrate ($Ca(NO_3)_2.4H_2O$) (Merk, Germany), magnesium chloride hexahydrate ($MgCl_2{\cdot}6H_2O$) (Merk, Germany), and tetraethyl orthosilicate ($(C_2H_5O)_4Si$, TEOS) (Merk, Germany). In brief, 0.25 mol of calcium nitrate tetrahydrate and 0.25 mol of $MgCl_2{\cdot}6H_2O$ were dissolved in 150 ml of ethanol, which served as the solvent. Subsequently, 0.50 mol of TEOS was added to the solution, and the mixture was stirred gently for 24 hours to facilitate wet gel formation. The resulting wet gel was dried in an air oven at 100 °C for 24 hours. The dried gel was then heated to 800 °C at a rate of 2 °C/min and maintained at this temperature for 2 hours. To produce the nanostructured diopside powder, the calcined powders were milled for 10 hours at a rotational speed of 250 rpm with a ball-to-powder ratio of 5/1, using a zirconia cup and balls [24].

2.2. Diopside scaffolds fabrication using the space holder method

In this method, spherical nanoparticle diopside powders were mixed with spacer particles. Sodium chloride particles, ranging in size from 420–600 μm, were used as the spacer material. The appropriate diopside powder to spacer ratios were selected based on the targeted degree of porosity to obtain the final porosities within 80% (i.e., 80 vol.% spacer and 20 vol.% diopside powder). The weight percentage of the spacer and powder was calculated using data from previous studies and according to Eq. (1) [13]:

$$w_{spacer} = \frac{V_{spacer} \times \rho_{spacer}}{(V_{spacer} \times \rho_{spacer} + V_{diopside} \times \rho_{diopside})} \times 100 \quad (1)$$

To maintain the sample height at the desired value, Eq. (2) was used to calculate the required amount of spacer and diopside powder:

$$\rho_T = \rho_{diopside} \times V_{diopside} + \rho_{spacer} \times V_{spacer} \quad (2)$$

Where ρ_T is the total density of the sample, V_{spacer} and $V_{diopside}$ are the volume fractions of the spacer and diopside, respectively, and ρ_{spacer} and $\rho_{diopside}$ are the densities of the spacer and diopside. The total density of the sample is calculated using Eq. (2), and by knowing the sample volume, the total weight can be derived from the density relation ($\rho = m/V$) [25].

After determining the appropriate ratios, diopside powder was mixed with spacer particles and homogenized using amalgamators. To maintain uniformity and reduce the pressing pressure, 2 wt.% food-grade sunflower oil was added to the mixture. The sunflower oil serves as an inspiration for the pore structure design, rather than interacting physically with the diopside material during pressing. This bioinspired design can lead to more efficient scaffold architectures, potentially reducing the required pressure during fabrication. The appropriate amounts of the mixture were then pressed into cylindrical molds with inner diameters of 6 and 13 mm using a universal testing machine (HOUNSFIELD: H50KS). Uniaxial pressing was conducted with an applied pressure of 50 MPa [25].

The cold-compacted cylindrical scaffolds were heated at a rate of 4 °C/min to 1200 °C and sintered at this temperature for 150 min. After sintering, the samples were soaked in double-distilled water (DDW) for 24 hours to remove NaCl particles [26].

2.3. Coating the polymeric phase inside the prepared scaffolds

To coat the polymeric phase in the bio-ceramic scaffolds, gelatin powder (2.5%, 5%, 7.5%, and 10% w/w) was dissolved in water, and the scaffolds were immersed in the solution under vacuum. After removing excess solution, the scaffolds were dried at ambient temperature. To increase the thickness of the polymeric coating, the immersion in the polymeric solution was repeated twice. Finally, the coated scaffolds were immersed in a 0.075 molar 1-Ethyl-3-(3-dimethyl aminopropyl) carbodiimide (EDC) solution in 90% ethanol and 10% double-distilled water (v/v) at 4 °C for 24 hours. The scaffolds were then washed with phosphate buffered saline (PBS) and dried at ambient temperature [27].

2.4. Evaluation and characterization of powders and produced scaffolds

2.4.1. Scanning electron microscopy analysis

Scanning electron microscopy (SEM, Phillips XL 30: Eindhoven, The Netherlands) was used to observe the morphology, size, shape, and interconnectivity of the pores in the scaffolds. The samples were gold-coated for enhanced resolution and observed at an accelerating voltage of 15 kV.

Pore size distribution was calculated by measuring the diameters of a minimum of 100 pores using an image analysis method. Scanning electron microscopy was also used to determine the formation of apatite and the morphology of the formed apatite on the scaffold surface after immersion in simulated body fluid (SBF). Additionally, the morphology and distribution of osteoblast cells on the scaffold surface were studied using SEM after the cell adhesion test [28].

2.4.2. Chemical composition analysis by energy-dispersive X-ray spectroscopy (EDS)

To determine the chemical composition of the produced powders and confirm the formation of apatite on the scaffold surface after immersion in SBF, energy-dispersive X-ray spectroscopy (EDS) analysis was performed using the SEM [28, 29].

2.4.3. Porosity measurement

The porosity of the prepared scaffolds was measured according to Archimedes' principle and in accordance with the ASTM B962 standard. For this purpose, three scaffolds' samples with different combinations, types, and percentages of space holder agents were selected, and the mean values obtained for porosity were reported. The porosity in the scaffolds is characterized by both open and closed forms. Open porosity, also known as visible porosity, determines the extent of the scaffold's permeability or the ease with which liquids and gases pass through it. This is calculated using Eq. (3), where W_d is the weight of the sample in air, W_s is the weight of the sample suspended in water, and W_w is the weight of the sample with water [30]:

$$Interconnected\ porosity = \frac{W_w - W_d}{W_w - W_s} \times 100 \quad (3)$$

The total porosity of the scaffolds, including both interconnected and closed pores, can be expressed by Eq. (4), where ρ is the actual or theoretical density of the diopside, which is equal to 3.26 g/cm^3.

$$Total\ porosity = \left(1 - \frac{W_d}{\rho(W_w - W_s)}\right) \times 100 \quad (4)$$

Additionally, the total porosity of the scaffold was calculated using Eq. (4), which involved measuring the diameter and height of the scaffolds with a digital caliper and determining the mass of the samples with a digital balance. The value of green density (ρ_g) was determined, as shown in Eq. (5), where ρ_g is the green density of the scaffolds and ρ is the actual or theoretical density of the diopside [30].

$$Total\ porosity = \left(1 - \left(\frac{\rho_g}{\rho}\right)\right) \times 100 \quad and \quad \rho_g = \frac{W_d}{\pi r^2 h} \quad (5)$$

The results were reported as the average of three scaffolds for each type of spacer, the volume fraction of spacer, and compaction pressure.

2.4.4. Mechanical strength testing

To evaluate the mechanical properties of diopside scaffolds, a compression test was conducted according to ASTM D5024 95a. Cylindrical specimens were produced using both gel and spray-pressed plastering methods, and the pressure test was performed using a universal test machine (Zwick, material prufung, 144660) [31].

The compressive strength of the sintered cylindrical samples (6 mm in diameter and 9 mm in height) with different porosities was tested using the testing machine at a crosshead speed of 0.5 mm/min. The samples were placed on the bottom ram of the machine, and the load was applied when the top ram moved downward. The compressive strength is defined as the fracture point recorded during the test divided by the original area. Five

scaffolds were used for testing to obtain average values [32]. The toughness of diopside scaffolds with different weight percentages of gelatin coating was determined by the area under the stress-strain curve obtained during the compression test until the fracture point. This represents the energy absorbed by the material before failure. Stiffness refers to the resistance to deformation when forces are applied and is defined as the ratio of stress to strain within the elastic region of the stress-strain curve [12].

2.4.5. Bioactivity and biodegradability evaluation

To evaluate the bioactivity, diopside scaffolds were immersed in the simulated body fluid (SBF). SBF has an ionic composition and pH similar to that of human blood plasma, making it widely used to simulate in vitro studies with in vivo studies. The immersion test in SBF was performed according to the ASTM G31 72 standard. The scaffolds were placed in polyethylene containers (15 cm), and SBF was added after the temperature reached 37 °C. The bottle caps were then blocked with plastic caps [33].

To ensure even precipitation of apatite on the surface, the specimens were immersed vertically in the SBF. The bottles were then placed in a bath at 36.5 ± 0.5 °C for different periods (7, 14, 21, and 28 days). For the preparation of SBF, two solutions, A and B, were prepared separately. First, 800 ml of water was distilled twice in two test tubes and heated to 37 °C in a magnetic stirrer [34].

Afterward, 0.934 ml of 1 molar hydrochloric acid was added to each of the two test tubes labeled A and B and allowed to dissolve completely in water. High-purity reagents listed in Table 1 were then added to solutions A and B. It should be noted that after the addition of each, sufficient time was allowed for the salt to dissolve completely in the solution. Finally, 200 ml of water (DDW) was added twice to each of the two test tubes [8].

Prior to sample immersion, solutions A and B were mixed, the temperature was equilibrated to 37 °C, and the pH was verified. After the predetermined immersion period, samples were removed from the SBF, rinsed with deionized water, and dried at ambient temperature. The sample surfaces were analyzed for apatite formation and pore filling by calcium phosphate compounds using SEM equipped with energy-dispersive X-ray spectroscopy (EDX) [35].

2.4.6. Evaluation of cytotoxicity, cell adhesion and alkaline phosphatase activity

Biocompatibility tests are designed to determine the ability of materials to maintain and restore the functionality of cells and tissues. One of the most well-known tests is the evaluation of cell viability through cell culture assays. Cell culture can be used to study cell responses to various stimuli, the production of therapeutic proteins such as bone marrow protein, cell response to various stimuli, the production and differentiation of different cells, the evaluation of how other substances affect the cell, gene therapy, and gene transfer. In all these cases, the number of cells and the number of living cells are counted [36, 37].

2.4.7. Evaluation of cell viability and cell proliferation

In this study, human osteoblast-like cells (SAOS 2) were obtained from the Pasteur Institute of Iran, and the tests were performed according to the ISO 10993 standard [38]. The cells were incubated at 37 °C in a medium containing RPMI 1640 with 10% fetal bovine serum (FBS) (Roswell Park Memorial Institute 1640). The second to third passage cells were detached using ethylenediaminetetraacetic acid (EDTA)-trypsin and 10^5 cells were added to the scaffolds for incubation at 37 °C [39].

Before exposure to the cells, the scaffolds were exposed to ultraviolet radiation for 30 minutes. At intervals of 1, 3, and 7 days, with the culture medium being changed every three days, the survival and proliferation of the cells were evaluated using the MTT assay [28, 40].

For this purpose, a solution of 5 mg/ml of MTT in PBS was prepared. 100 µl of this solution, along with 500 µl of RPMI medium, was added to the specimens and incubated at 37 °C for 4 hours. After incubation, the culture medium containing MTT was removed, and the scaffolds were washed twice with PBS. The medium was

then replaced with 400 µl of DMSO solution, and the scaffolds were left for 30 minutes to dissolve the formazan. The absorbance of light was measured at 570 nm using 50 µl of the obtained solution. As a negative control, SAOS2 cells were cultured in wells without scaffolds [30, 39].

For the positive control, SAOS2 cells were cultured with culture medium containing 0.2% Triton. One of the problems in examining the amount of cell viability and proliferation by MTT in the vicinity of the scaffolds is the absorption of color by the scaffolds, which can lead to errors in the results. To address this, a scaffold was placed in the controlled well during the addition of MTT, ensuring the same condition for color absorption between the control sample and other specimens [29, 42].

2.4.8. Survey of cell adhesion

The fabricated scaffolds, after sterilization, were exposed to ultraviolet light in 24-well cell culture plates. Then, 800 µl of the medium containing RPMI 1640-10% FBS and 10^5 osteoblast cells were added to the specimens and incubated at 37 °C. After 3 and 7 days (with the culture medium being changed every 3 days), the culture medium was removed and the scaffolds were washed twice with PBS. The specimens were then stabilized at 700 µl of a 2.5% glutaraldehyde solution for 1 hour. Afterward, the scaffolds were rewashed with PBS and dehydrated in ethanol solutions with increasing concentrations (30%, 50%, 70%, 90%, 95%, and 100%) for about 15 minutes at each concentration. The scaffolds were then placed under the hood to dry. After drying, the samples were mounted on copper bases, coated with gold, and observed using scanning electron microscopy (SEM) [29, 33].

2.4.9. Alkaline phosphatase analysis

Alkaline phosphatase activity is a parameter for osteoblastic activity. For this purpose, an alkaline phosphatase assay kit was used. The fabricated scaffolds, after sterilization, were exposed to ultraviolet light in 24-well cell culture plates. Then, 800 µl of the medium containing RPMI 1640-10% FBS and 10^5 of the osteoblast cells were added to the specimens and incubated at 37 °C and 5% CO_2. After 3 and 7 days (with the culture medium being changed every 3 days), the culture medium was removed, and the scaffolds were washed twice with PBS. The cells on the scaffolds were then lysed for 1 hour using 100 µl of 0.2% Triton Lysing solution for each scaffold. Two microliters of the cell lysis solutions were mixed with 100 µl of an 80% solution of 10 mM p-nitrophenyl phosphate, 20% of 1 mM diethanolamine, and 0.5 mM magnesium chloride solution. After incubation at 37 °C for 30 minutes, the reaction was stopped by adding 0.1% NaOH, and absorbance at 405 nm was measured using a spectrophotometer [32, 41].

The total protein content was measured using a total protein kit. For this purpose, 2 µl of the solution obtained from cell destruction was mixed with 100 µl of a reagent solution containing 30 mM potassium iodide, 32 mM potassium sodium tartrate, 18 mM copper sulfate, and 200 mM sodium hydroxide. After incubation at 37 °C for 20 minutes, absorbance at 546 nm was measured using a spectrophotometer. The activity of alkaline phosphatase was then calculated as the number of nanomoles of p-nitrophenyl phosphate converted per minute per milligram of total protein, based on the concentration of p-nitrophenyl phosphate and total protein. As a control, SAOS2 cells were cultured in wells without any scaffolds [32, 39].

Table 1. The amounts of chemical reagents needed to make the two SBF solutions

Materials	Solution A	Solution B	Chemical formula
Hydrochloric acid	0.934 ml	0.934 ml	1 M - HCl
Sodium chloride	6.129 g	6.129 g	NaCl
Sodium hydrogen carbonate	5.890 g	---	$NaHCO_3$
Sodium hydrogen phosphate dihydrate	0.498 g	---	$Na_2HPO_4.2H_2O$
Calcium chloride	---	0.540 g	$CaCl_2$

2.5. Statistical analysis

Each experiment was conducted in triplicate, and the resulting data were analyzed using the Statistical Package for the Social Sciences (SPSS) software. Statistical significance among various groups was assessed using one-way ANOVA and the t-test. The Tamhane post hoc test was employed to identify differences between specific groups. A p-value ≤ 0.05 was considered statistically significant, indicating meaningful differences [42].

3. Results and Discussion

3.1. Analysis of SEM images of diopside scaffold after coating with gelatin at different concentrations

Figs. 1 to 4 present SEM images of diopside scaffolds produced with 80 vol.% sodium chloride as a space holder and compacted at 50 MPa, following coating with gelatin solutions of 2.5%, 5%, 7.5%, and 10% (w/w) at varying magnifications. The images clearly demonstrate that the polymeric gelatin coating does not significantly affect the morphology and porosity of the scaffolds compared to the uncoated ones. The method employed in this study results in a thin layer of polymeric phase on the pore walls while simultaneously creating a polymeric layer at the boundaries and filling in the microporosity within the walls. This process leads to a reduction in the overall porosity of the scaffolds. Furthermore, the images reveal that increasing the gelatin solution concentration results in a greater amount of microporosity on the cavity walls and a reduction in porosity correlation. Notably, the high degradability of the selected polymer in simulated body fluids is significant, as it has the potential to reopen the microporosities. This degradability, in combination with the polymer's other chosen properties, may further enhance the scaffold's suitability in bone tissue engineering.

As evident from the figures, the gelatin polymer coating facilitates the bridging of ceramic phase particles and the filling of micropores and microcracks in the scaffold. This phenomenon enhances the scaffold's strength and notably reduces the brittleness typically associated with ceramic scaffolds. These improvements are further discussed in the section on mechanical property evaluation. The average values for total porosity and open porosity of diopside scaffolds, prepared using 80 vol.% sodium chloride powder as a space holder and pressed at 50 MPa, with varying weight percentages of gelatin coating, are shown in Table 2. As shown, increasing the gelatin concentration leads to a decrease in both total porosity and open porosity percentages.

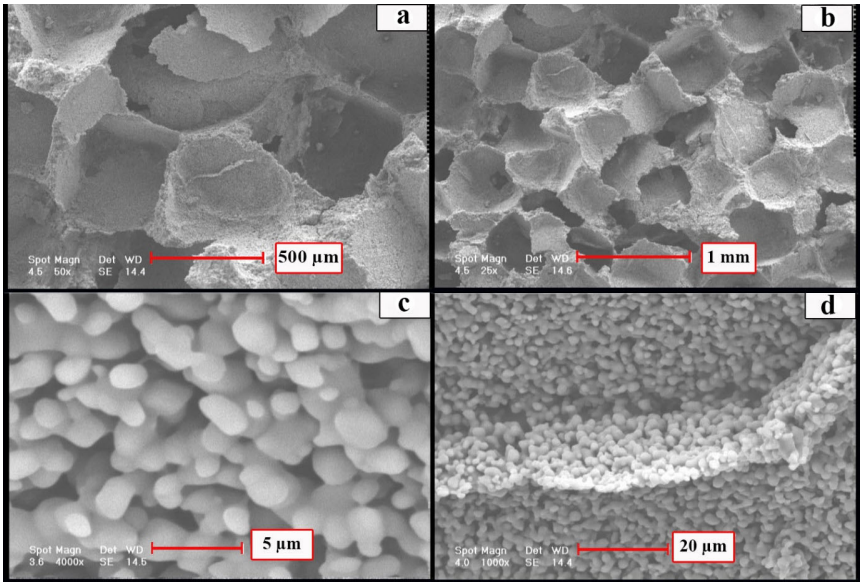

Fig. 1. SEM of diopside scaffold after coating with 2.5 wt.% gelatin: (a) 50x magnification, (b) 25x magnification, (c) 4000x magnification, and (d) 1000x magnification.

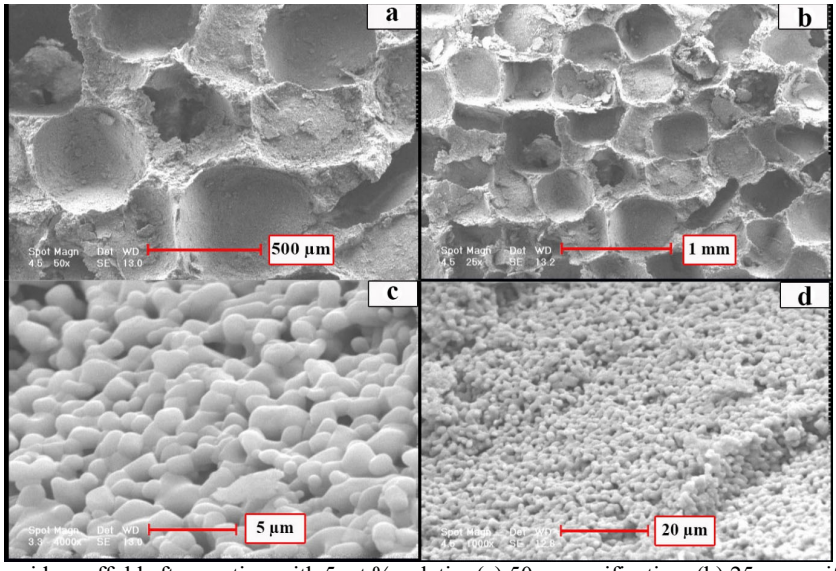

Fig. 2. SEM of diopside scaffold after coating with 5 wt.% gelatin: (a) 50x magnification, (b) 25x magnification, (c) 4000x magnification, and (d) 1000x magnification.

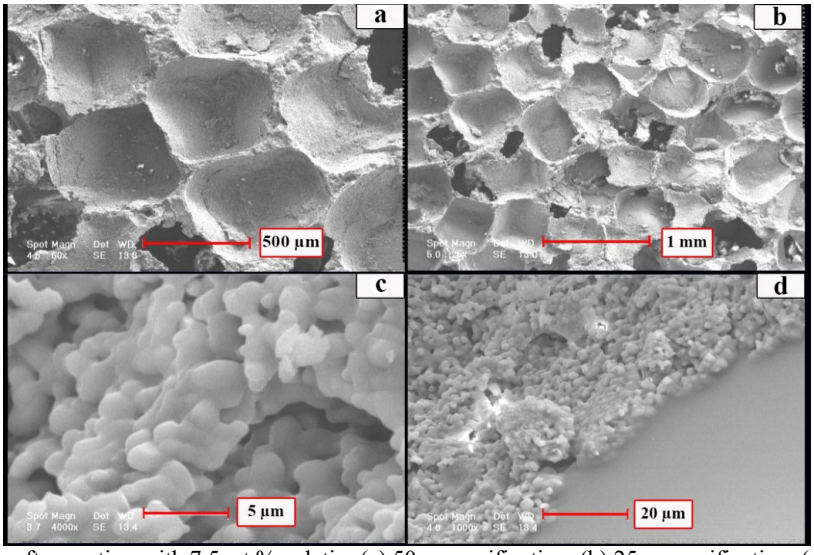

Fig. 3. SEM of diopside after coating with 7.5 wt.% gelatin: (a) 50x magnification, (b) 25x magnification, (c) 4000x magnification, and (d) 1000x magnification.

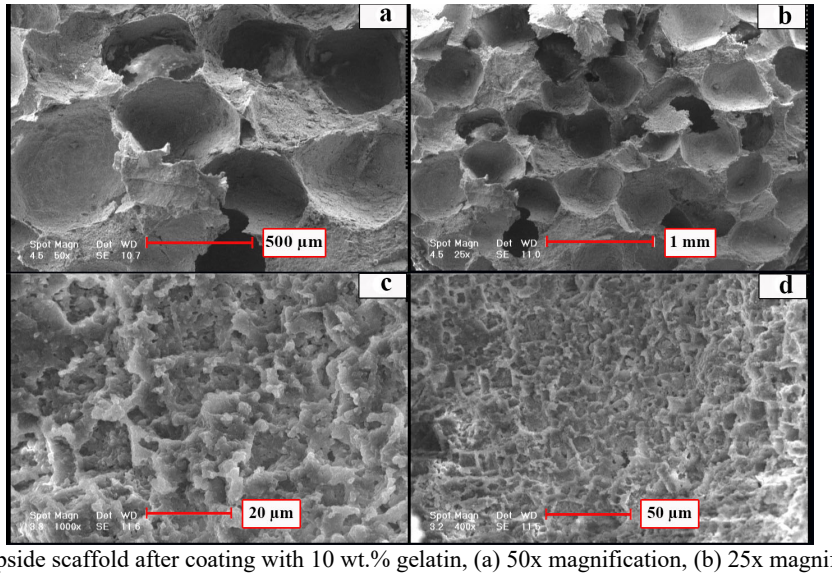

Fig. 4. SEM of diopside scaffold after coating with 10 wt.% gelatin, (a) 50x magnification, (b) 25x magnification, (c) 4000x magnification, (d) 1000x magnification.

Table 2. Total porosity and open porosity values for scaffolds prepared by powder pressing with 80 vol.% sodium chloride as a space holder, under 50 MPa pressure, and with different weight percentages of gelatin coating (values in parentheses represent deviations from the standard)

Weight percent gelatin	Total porosity (%)	Open porosity (%)
0% (w/w)	85 (±1.2)	82 (±2.5)
2.5% (w/w)	82 (±2)	76 (±3)
5% (w/w)	78 (±1.5)	73 (±2)
7.5% (w/w)	75 (±1)	57 (±1.2)
10% (w/w)	70 (±1)	45 (±1.4)

3.2. Effect of gelatin coatings on total open porosity

Gelatin coatings effectively reduce the open porosity of scaffolds. A 10% (w/w) gelatin coating resulted in an approximately 15% decrease in total porosity while significantly reducing open porosity by 40%. This indicates that the polymer coating primarily fills micro-cavities within the porous structure, thereby impacting open porosity more substantially than total porosity. Considering the importance of porous structure with open porosity for tissue engineering applications, scaffold coated with 5% (w/w) gelatin showed better open porosity, making them more suitable for bone tissue engineering. Fig. 5 illustrates the total and open porosity values for diopside scaffolds with different weight percentages of gelatin coating.

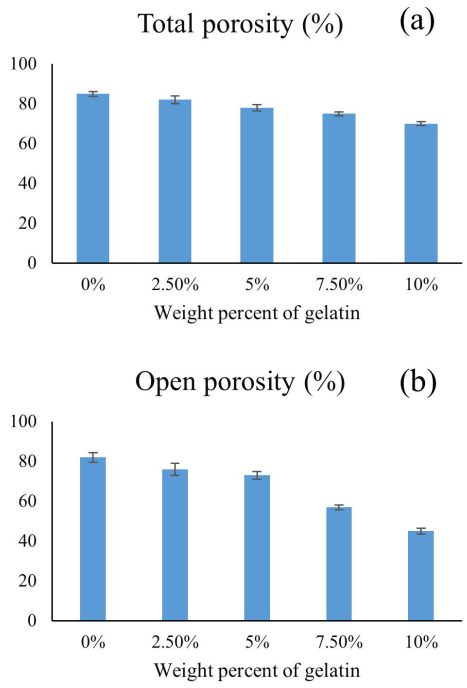

Fig. 5. (a) Total and (b) open porosity values for diopside scaffolds with different weight percentages of gelatin coating.

3.3. Compressive strength, stiffness, and toughness of composite diopside scaffolds

The average values for compressive strength, stiffness, and toughness of diopside scaffolds prepared via the powder pressing method using 80 vol.% sodium chloride as a space holder, under 50 MPa pressure and with different weight percentages of gelatin coating, are summarized in Table 3. Compressive strength is defined as the maximum stress a scaffold can endure before failure, which is determined by the peak point on the stress-strain curve.

The results demonstrate a positive correlation between the gelatin concentration and both the compressive strength and elastic modulus, accompanied by a reduction in porosity. Toughness, calculated as the area under the stress-strain curve up to the failure point, also shows significant improvement with increasing gelatin concentration. For instance, with a 2.5 wt.% gelatin solution, the toughness was approximately 3.4 times greater, and at 10% gelatin concentration, it was enhanced nearly 18 times. The observed increase in strength and toughness of the scaffolds due to the application of polymeric gelatin coatings can be attributed to several factors.

Table 3. Toughness, compressive strength, and stiffness values for diopside scaffolds with different weight percentages of gelatin coating

Weight percent gelatin	Compressive strength (MPa)	Stiffness (MPa)	Toughness ($\mu j/m^3$)
0	0.98±0.11	68±7	71.35±19.16
2.5	2.14±0.08	106±7	242.84±21.32
5	3.27±0.16	118±6	405.36±40.82
7.5	3.78±0.05	133±7	822.58±32.41
10	4.62±0.09	146±12	1248.38±68.21

The first factor is the reduction of porosity achieved through the application of polymer coatings. Applying a polymer coating with 10 wt.% gelatin can reduce total porosity by approximately 15%. The second factor involves the filling of microporosities and the probable microcracks within the pore walls. These microporosities often serve as stress concentration points, initiating cracking. By filling these

microporosities, these microporosities, stress concentrations are reduced, and the micro-walls are effectively bridged, preventing crack propagation in the scaffold. The third factor contributed to improved mechanical properties is the more uniform distribution observed in scaffolds with polymeric compared to uncoated scaffolds.

The compressive strength is defined as the maximum stress the scaffold can endure before reaching the failure point, determined from the peak of the stress-strain curve. The toughness of diopside scaffolds with different weight percentages of gelatin coating is determined from the area under the stress-strain curve obtained during a compression test up to the failure point. This parameter represents the energy absorbed by the material before failure and is particularly significant for brittle materials like diopside scaffolds, where fracture toughness is a critical factor. Stiffness, on the other hand, refers to the material's resistance to deformation under applied forces. It is quantified as the ratio of stress to strain in the elastic region of the stress-strain curve, indicating the rigidity of the scaffold material.

Fig. 6 shows that the non-coated scaffolds behaved similarly to brittle porous materials [43]. The stress-strain diagrams consist of three regions. The first one exhibits linear elongation, which ends with the first cracks in the sample, corresponding to the maximum compressive strength. Region Two shows a gradual destruction of the walls and porosity, leading to the collapse of the scaffold walls and partial fracture. Region Three shows the strength of the compressed scaffold, and for this reason, an increase in strength can be seen in the stress-strain graphs. Also, as shown in Table 3, coating the scaffolds with gelatin polymer and increasing the gelatin weight percentage significantly improves the strength and toughness of the scaffolds. In this study, toughness values were measured up to the fracture point on the curve, showing that polymer coatings enhanced toughness, with a marked increase in toughness as the gelatin solution concentration rose.

Typical stress-strain diagrams for diopside scaffolds, prepared and coated with solutions with different weight percentages of gelatin are shown in Fig. 6. Bone tissue is strong and forms one of the body's rigid structures due to the combination of organic and inorganic materials. It is a viscoelastic and adaptable material that is highly sensitive to inappropriate use, lack of mobility, excessive activity, and high-load levels. Its mechanical properties depend on factors such as the type of bone, the nature and direction of loading, as well as an individual's activity and nutrition. The collagen polymeric phase creates the properties of bone resilience and the ability to withstand tensile forces. Bone is also a brittle material, with its degree of fragility depending on the mineral compounds present, which allow it to endure compressive loads. Creating a composite scaffold of ceramic and gelatin can increase bone resemblance, producing a structure with bone-like toughness and strength. In bone tissue engineering, ideal scaffolds typically have about 80 to 90 percent porosity. However, achieving such high porosity in ceramic and polymer scaffolds often results in a significant decrease in mechanical properties, which limits their use in load-bearing applications. For scaffolds intended for load-bearing purposes, fracture plates may be necessary as supports. While it is highly desirable, but not essential, for scaffolds to have mechanical properties similar to the host tissue. Studies have shown that internal bone growth can improve compressive strength. For instance, Yoshikawa et al. [44] reported that the compressive strength of porous hydroxyapatite increased from 2 MPa to 20 MPa after three months of implantation. Considering that bone compression strength ranges from 100 to 230 MPa and spongy bone's compressive strength is about 2 to 12 MPa, scaffolds with higher compressive strength are more suitable for use in bone tissue engineering.

In bone tissue engineering, the strength of a scaffold is an important characteristic, as it must withstand forces during surgery and provide mechanical stability at the load-bearing site until new tissue regenerates. The scaffolds produced in this study were able to withstand forces during bioactivity and cell culture tests. Furthermore, their compressive strength, falling within the range reported by Gibson and Ashby [45] (0.2 to 4 MPa) for spongy bone with 90% porosity, highlights

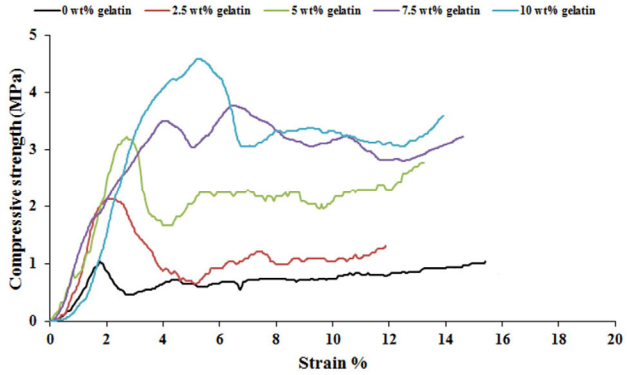

Fig. 6. Stress-strain diagrams of typical diopside scaffolds produced and coated with different weight percentages of gelatin solutions.

their potential for load-bearing applications in bone tissue engineering.

Scanning electron microscopy (SEM) analysis of the diopside scaffold, prepared by powder pressing and coated with a 5% gelatin solution, followed by immersion in simulated body fluid (SBF) for 28 days, revealed notable changes in the scaffold's surface morphology. Before immersion, the diopside scaffolds exhibited a relatively rough surface, with visible interparticle boundaries typical of the fabrication method. The gelatin coating appeared as a smoother layer over the rough substrate, potentially filling some of the interparticle spaces and modifying the overall surface texture. As shown in Fig. 7, after 28 days of immersion in SBF, mineralization and degradation processes were observed on the scaffold surface.

3.4. Investigation of the chemical composition of surface sediments to confirm the formation of apatite by EDS

Elemental analysis using EDS was used to investigate the chemical composition and confirm the formation of apatite on the surface of diopside and bredigite production.

Figs. 8 to 10 represent the regional spectra of the prepared scaffolds after immersion in SBF. The spectra of scaffolds post-immersion indicate the presence of the phosphorus element, which together with the calcium, confirms the formation of calcium phosphate compounds on the surface. To further verify the precipitation of phosphorus after immersion in SBF, the spectrum of the diopside scaffold before immersion is also shown in Fig. 10. As observed, phosphorus is present in the diopside scaffold prior to immersion in SBF.

3.5. Cell viability and cell toxicity by MTT assay

The viability and cytotoxicity of osteoblast cells cultured on diopside scaffolds were evaluated using the MTT assay. The scaffolds, both with and without gelatin coating, were assessed after 1, 3, and 7 days of cell culture and compared to a post-culture control. Fig. 11 presents the results demonstrating the effect of gelatin coating at different concentrations on osteoblast viability over time. Fig. 12 shows scanning electron microscopy (SEM) images depicting the morphology and attachment of osteoblast cells cultured on a diopside scaffold coated with a 5 wt.% gelatin solution. Figs. 12(a) and 12(b) display cell behavior after 3 days of culture, while 12(c) and 12(d) show the cells after 7 days. These images allow for the comparison of cell morphology, spreading, and proliferation on the gelatin-coated diopside scaffold over time. Notable differences in cell density, cell-material interaction, and extracellular matrix deposition are observed between the two time points, providing insights into the biocompatibility and osteoconductivity of the scaffold.

3.6. Investigation of alkaline phosphatase (ALP) activity

This study aims to investigate the impact of gelatin coating on the osteogenic differentiation of cultured osteoblast cells cultured on diopside scaffolds. Alkaline phosphatase (ALP) activity, a marker of osteoblast differentiation, was measured after 3 and 7 days of culture on scaffolds coated with 2.5 wt.% and 5 wt.% gelatin solutions, as well as on uncoated control scaffolds.

The results suggest that 5 wt.% gelatin coating enhances the early osteogenic differentiation of osteoblasts on diopside scaffolds, potentially improving their biocompatibility and bone-forming capacity for use in bone tissue engineering applications.

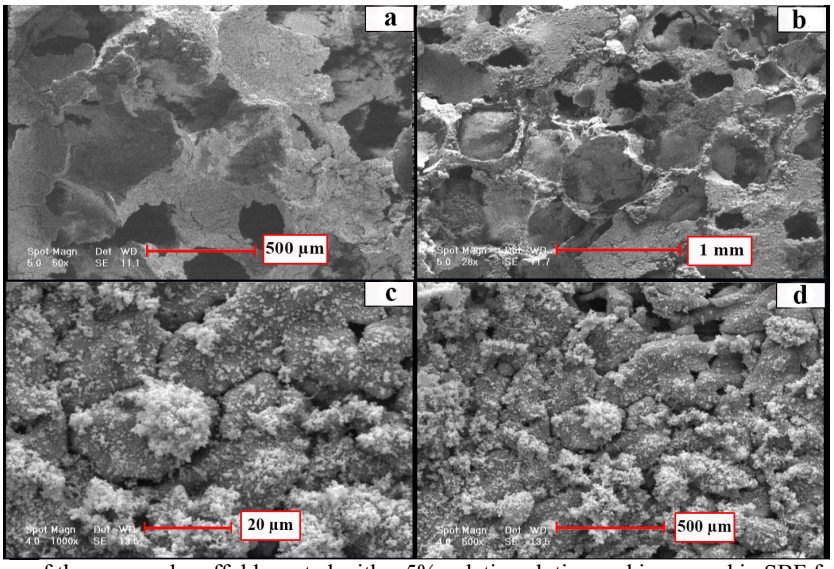

Fig. 7. SEM images of the prepared scaffold, coated with a 5% gelatin solution and immersed in SBF for 28 days: (a) 50x magnification, (b) 28x magnification, (c) 1000x magnification, and (d) 500x magnification.

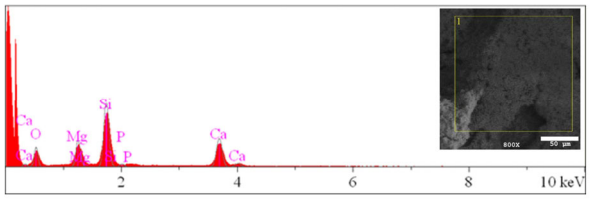

Fig. 8. Regional spectral analysis of EDS of prepared diopside scaffolds after immersion in SBF for 28 days.

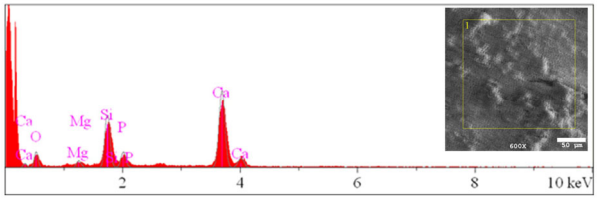

Fig. 9. Regional spectral analysis of EDS of prepared diopside scaffolds coated with 5 wt.% gelatin solution after immersion in SBF for 28 days.

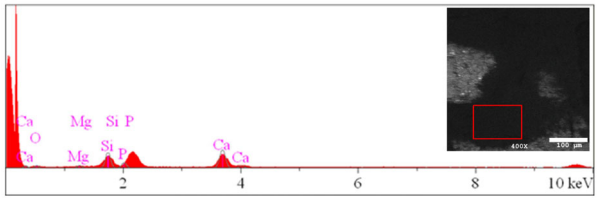

Fig. 10. Regional spectral analysis of EDS of prepared diopside scaffolds before immersion in SBF for 28 days.

Alkaline phosphatase (ALP) activity is a crucial indicator of osteoblast differentiation and bone formation, making it a key parameter for evaluating

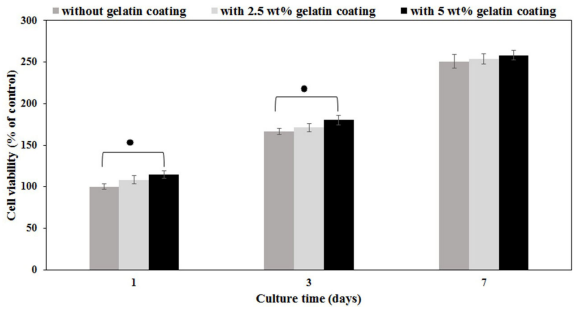

Fig. 11. Percentage of osteoblast cell viability on diopside scaffolds coated with 2.5 and 5 wt.% gelatin solutions, as well as uncoated scaffolds, compared to post-culture control after 1, 3, and 7 days of cell culture.

the bioactivity of bone tissue engineering scaffolds. When assessing diopside scaffolds coated with gelatin, measuring ALP activity provides valuable insights into how the gelatin coating influences the scaffold's ability to support bone regeneration. Specifically, investigating ALP activity in diopside scaffolds coated with 5 wt.% gelatin helps identify the optimal gelatin concentration for promoting osteogenic differentiation. The ALP activity of osteoblast cells cultured on scaffolds coated with 2.5 and 5 wt.% gelatin solutions, as well as uncoated scaffolds, after 3 and 7 days, is shown in Fig. 13.

Higher ALP activity suggests a more favorable environment for bone cell growth and mineralization.

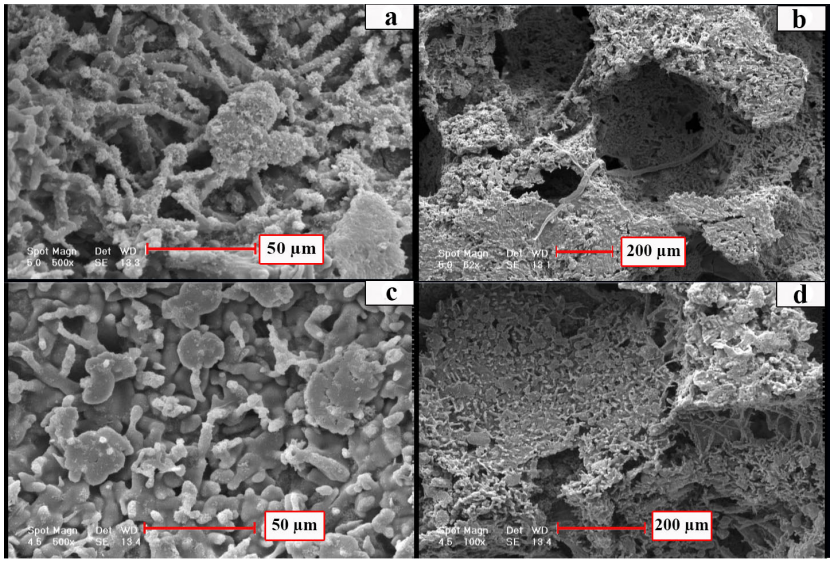

Fig. 12. SEM images of osteoblast cells cultured on a diopside scaffold coated with a 5 wt.% gelatin solution after (a) 3 days in 500x magnification, (b) 3 days in 52x magnification, (c) 7 days in 500x magnification, (d) 7 days in 100x magnification.

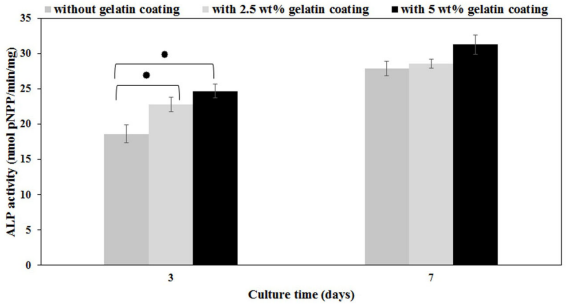

Fig. 13. Alkaline phosphatase activity of osteoblast cells cultured on prepared scaffolds coated with 2.5 and 5 wt.% gelatin solutions, as well as uncoated scaffolds after 3 and 7 days of culture.

Comparing the ALP activity at different gelatin concentrations highlights the dose-dependent effects of gelatin on osteoblast function and ultimately, bone tissue formation. This information is crucial for optimizing the design and fabrication of diopside-gelatin composite scaffolds for bone repair and regeneration applications.

4. Conclusion

This study investigated the fabrication and characterization of novel diopside-gelatin composite scaffolds for bone tissue engineering applications. The scaffolds were fabricated using a salt-leaching technique with 80 vol.% sodium chloride as a porogen. Subsequently, the resulting diopside scaffolds were coated with varying concentrations (2.5%, 5%, 7.5%, and 10 wt.%) of gelatin solution under a uniaxial pressure of 50 MPa. This approach capitalizes on the combined benefits of polymer-coated ceramic scaffolds in bone tissue engineering. Determining the optimal gelatin concentration, identified as 5% w/w, remains complex and requires further investigation through various tests. Future in vivo studies and clinical trials are recommended to validate the efficacy of these scaffolds for bone tissue regeneration.

Analysis of the fabricated scaffolds revealed that a 5 wt.% gelatin coating yielded optimal properties, specifically superior open porosity compared to other coating concentrations. The synergistic combination of diopside ceramic and gelatin polymer within the scaffold structure is hypothesized to enhance key bone-like properties, including toughness and compressive strength. The gelatin coating serves as a binder, improving the interconnectivity of the diopside particles while filling microporosities, contributing to the enhancement of mechanical properties.

The findings suggest that the diopside-gelatin composite scaffolds with a 5 wt.% gelatin coating hold promise for bone tissue regeneration. However, further investigation is needed to fully evaluate their biocompatibility and osteoconductive potential. Future research should include in vitro studies assessing cell attachment, proliferation, and differentiation, followed by in vivo studies evaluating bone formation in relevant

animal models. Successful preclinical results could pave the way for clinical trials, enabling the translation of these composite scaffolds into therapeutic solutions for bone defects and injuries. Overall, the results indicate that these composite scaffolds are suitable for engineered bone tissue, and further investigation, including in vivo studies and clinical trials, is strongly recommended.

Author contributions

All authors contributed extensively to the work presented in this paper.

Conflict of interest

The authors declare that there is no conflict of interest in this research.

Funding

The authors declared that no grants were involved in supporting this work.

5. References

[1] Black, C. R., Goriainov, V., Gibbs, D., Kanczler, J., Tare, R. S., & Oreffo, R. O. (2015). Bone tissue engineering. *Current Molecular Biology Reports*, *1*(3), 132-140. https://doi.org/10.1007/s40610-015-0022-2

[2] Amini, A. R., Laurencin, C. T., & Nukavarapu, S. P. (2012). Bone tissue engineering: recent advances and challenges. *Critical Reviews™ in Biomedical Engineering*, *40*(5). https://doi.org/10.1615/critrevbiomedeng.v40.i5.10

[3] Lee, S. S., Du, X., Kim, I., & Ferguson, S. J. (2022). Scaffolds for bone-tissue engineering. *Matter*, *5*(9), 2722-2759. https://doi.org/10.1016/j.matt.2022.06.003

[4] Razavi, M., Fathi, M., Savabi, O., Beni, B. H., Vashaee, D., & Tayebi, L. (2014). Surface microstructure and in vitro analysis of nanostructured akermanite ($Ca_2MgSi_2O_7$) coating on biodegradable magnesium alloy for biomedical applications. *Colloids and Surfaces B: Biointerfaces*, *117*, 432-440. https://doi.org/10.1016/j.colsurfb.2013.12.011

[5] Sharafabadi, A. K., Abdellahi, M., Kazemi, A., Khandan, A., & Ozada, N. (2017). A novel and economical route for synthesizing akermanite ($Ca_2MgSi_2O_7$) nano-bioceramic. *Materials Science and Engineering: C*, *71*, 1072-1078. https://doi.org/10.1016/j.msec.2016.11.021

[6] Kanwar, S., & Vijayavenkataraman, S. (2021). Design of 3D printed scaffolds for bone tissue engineering: A review. *Bioprinting*, *24*, e00167. https://doi.org/10.1016/j.bprint.2021.e00167

[7] Wu, C., Chang, J., Zhai, W., Ni, S., & Wang, J. (2006). Porous akermanite scaffolds for bone tissue engineering: preparation, characterization, and in vitro studies. *Journal of Biomedical Materials Research Part B: Applied Biomaterials*, *78*(1), 47-55. https://doi.org/10.1002/jbm.b.30456

[8] Rafiee, N., Karbasi, S., Nourbakhsh, A. A., & Amini, K. (2022). Natural hydroxyapatite/diopside nanocomposite scaffold for bone tissue engineering applications: physical, mechanical, bioactivity and biodegradation evaluation. *Materials Technology*, *37*(1), 36-48. https://doi.org/10.1080/10667857.2020.1806189

[9] Nicoara, A. I., Alecu, A. E., Balaceanu, G. C., Puscasu, E. M., Vasile, B. S., & Trusca, R. (2023). Fabrication and characterization of porous diopside/akermanite ceramics with prospective tissue engineering applications. *Materials*, *16*(16), 5548. https://doi.org/10.3390/ma16165548

[10] Srinath, P., Abdul Azeem, P., & Venugopal Reddy, K. (2020). Review on calcium silicate-based bioceramics in bone tissue engineering. *International Journal of Applied Ceramic Technology*, *17*(5), 2450-2464. https://doi.org/10.1111/ijac.13577

[11] Zamani Foroushani, R., Karamian, E., & Rafienia, M. (2022). Evolution of biological properties of bioactive diopside and wollastonite for bone tissue engineering. *Journal of Advanced Materials and Processing*, *10*(1), 39-56. https://doi.org/10.21203/rs.3.rs-52269/v1

[12] Joseph, S., & Swamiappan, S. (2024). Preparation and characterization of diopside-wollastonite composite for orthopedic application. *Silicon*, *16*(3), 1161-1171. https://doi.org/10.1007/s12633-023-02737-4

[13] Healy, K., & Guldberg, R. (2007). Bone tissue engineering. *Journal of Musculoskeletal and Neuronal Interactions*, *7*(4), 328. https://doi.org/10.1089/ten.2006.0041

[14] Ahmadipour, M., Mohammadi, H., Pang, A. L., Arjmand, M., Ayode Otitoju, T., U. Okoye, P., & Rajitha, B. (2022). A review: silicate ceramic-polymer composite scaffold for bone tissue engineering. *International Journal of Polymeric Materials and Polymeric Biomaterials*, *71*(3), 180-195. https://doi.org/10.1080/00914037.2020.1817018

[15] Gkioni, C., Leeuwenburgh, S., & Jansen, J. (2020). Biodegradable polymeric/ceramic composite scaffolds to regenerate bone tissue. In S. Dumitriu & V. Popa (Eds.), *Polymeric Biomaterials* (pp. 239-260). CRC Press. https://doi.org/10.1201/b13757-9

[16] Barroso, G., Li, Q., Bordia, R. K., & Motz, G. (2019). Polymeric and ceramic silicon-based coatings–a review.

Journal of Materials Chemistry A, *7*(5), 1936-1963. https://doi.org/10.1039/c8ta09054h

[17] Subhapradha, N., Abudhahir, M., Aathira, A., Srinivasan, N., & Moorthi, A. (2018). Polymer coated mesoporous ceramic for drug delivery in bone tissue engineering. *International Journal of Biological Macromolecules*, *110*, 65-73. https://doi.org/10.1016/j.ijbiomac.2017.11.146

[18] Benedini, L., & Messina, P. (2024). Advances in polymer/ceramic composites for bone tissue engineering applications. In S. Kargozar & F. Baino (Eds.), *Bioceramics: Status in Tissue Engineering and Regenerative Medicine (Part 1)* (pp. 231-251). Bentham Science Publishers. https://doi.org/10.2174/9789815238396124010012

[19] Peroglio, M., Gremillard, L., Chevalier, J., Chazeau, L., Gauthier, C., & Hamaide, T. (2007). Toughening of bio-ceramics scaffolds by polymer coating. *Journal of the European Ceramic Society*, *27*(7), 2679-2685. https://doi.org/10.1016/j.jeurceramsoc.2006.10.016

[20] Reddy, M. S. B., Ponnamma, D., Choudhary, R., & Sadasivuni, K. K. (2021). A comparative review of natural and synthetic biopolymer composite scaffolds. *Polymers*, *13*(7), 1105. https://doi.org/10.3390/polym13071105

[21] Yang, Q., Zhao, J., Muhammad, A., Tian, L., Liu, Y., Chen, L., & Yang, P. (2022). Biopolymer coating for particle surface engineering and their biomedical applications. *Materials Today Bio*, *16*, 100407. https://doi.org/10.1016/j.mtbio.2022.100407

[22] Bikuna-Izagirre, M., Aldazabal, J., & Paredes, J. (2022). Gelatin blends enhance performance of electrospun polymeric scaffolds in comparison to coating protocols. *Polymers*, *14*(7), 1311. https://doi.org/10.3390/polym14071311

[23] Hayashi, S., Otsuka, N., Akiyama, K., Okada, K., & Yano, T. (1989). Preparation of diopside fine powders by spray pyrolysis and its sinterability. *Journal of the Ceramic Society of Japan*, *97*(1127), 742-746. https://doi.org/10.2109/jcersj.97.742

[24] Choudhary, R., Vecstaudza, J., Krishnamurithy, G., Raghavendran, H. R. B., Murali, M. R., Kamarul, T., Swamiappan, S., & Locs, J. (2016). In-vitro bioactivity, biocompatibility and dissolution studies of diopside prepared from biowaste by using sol–gel combustion method. *Materials Science and Engineering: C*, *68*, 89-100. https://doi.org/10.1016/j.msec.2016.04.110

[25] Sadeghzade, S., Emadi, R., Ahmadi, T., & Tavangarian, F. (2019). Synthesis, characterization and strengthening mechanism of modified and unmodified porous diopside/baghdadite scaffolds. *Materials Chemistry and Physics*, *228*, 89-97. https://doi.org/10.1016/j.matchemphys.2019.02.041

[26] Ramezani, S., Emadi, R., Kharaziha, M., & Tavangarian, F. (2017). Synthesis, characterization and in vitro behavior of nanostructured diopside/biphasic calcium phosphate scaffolds. *Materials Chemistry and Physics*, *186*, 415-425. https://doi.org/10.1016/j.matchemphys.2016.11.013

[27] Sayed, M., Mahmoud, E., Bondioli, F., & Naga, S. (2019). Developing porous diopside/hydroxyapatite bio-composite scaffolds via a combination of freeze-drying and coating process. *Ceramics International*, *45*(7), 9025-9031. https://doi.org/10.1016/j.ceramint.2019.01.236

[28] Teimouri, A., Roohafza, S., Azadi, M., & Chermahini, A. N. (2018). Fabrication and characterization of chitosan/gelatin/nanodiopside composite scaffolds for tissue engineering application. *Polymer Bulletin*, *75*(4), 1487-1504. https://doi.org/10.1007/s00289-017-2096-x

[29] Wahaia, F., Kasalynas, I., Karaliunas, M., Urbanowicz, A., Seifert, B., Valusis, G., & Ferraro, V. (2024). Effect of bone age and anatomy on the variability of the bovine bone by-product by Terahertz time-domain spectroscopy and energy-dispersive X-ray microanalysis. *Food Bioscience*, *59*, 103978. https://doi.org/10.1016/j.fbio.2024.103978

[30] Hosseini, Y., Emadi, R., & Kharaziha, M. (2017). Surface modification of PCL-diopside fibrous membrane via gelatin immobilization for bone tissue engineering. *Materials Chemistry and Physics*, *194*, 356-366. https://doi.org/10.1016/j.matchemphys.2017.03.051

[31] Pang, S., Wu, D., Yang, H., Kamutzki, F., Kurreck, J., Gurlo, A., & Hanaor, D. A. (2023). Enhanced mechanical performance and bioactivity in strontium/copper co-substituted diopside scaffolds. *Biomaterials Advances*, *145*, 213230. https://doi.org/10.1016/j.bioadv.2022.213230

[32] Shemshad, S., Kamali, S., Khavandi, A., & Azari, S. (2019). Synthesis, characterization and in-vitro behavior of natural chitosan-hydroxyapatite-diopside nanocomposite scaffold for bone tissue engineering. *International Journal of Polymeric Materials and Polymeric Biomaterials*, *68*(9), 516-526. https://doi.org/10.1080/00914037.2018.1466138

[33] Sobhani, A., & Salimi, E. (2023). Low temperature preparation of diopside nanoparticles: in-vitro bioactivity and drug loading evaluation. *Scientific Reports*, *13*(1), 16330. https://doi.org/10.1038/s41598-023-43671-0

[34] Goudouri, O., Theodosoglou, E., Kontonasaki, E., Will, J., Chrissafis, K., Koidis, P., Paraskevopoulos, K., & Boccaccini, A. (2014). Development of highly porous scaffolds based on bioactive silicates for dental tissue engineering. *Materials Research Bulletin*, *49*, 399-404. https://doi.org/10.1016/j.materresbull.2013.09.027

[35] Kordjamshidi, A., Saber-Samandari, S., Nejad, M. G., & Khandan, A. (2019). Preparation of novel porous calcium silicate scaffold loaded by celecoxib drug using freeze drying technique: Fabrication, characterization and simulation. *Ceramics International*, *45*(11), 14126-14135. https://doi.org/10.1016/j.ceramint.2019.04.113

[36] Moatary, A., Teimouri, A., Bagherzadeh, M., Chermahini, A. N., & Razavizadeh, R. (2017). Design and fabrication of novel chitin hydrogel/chitosan/nano diopside composite scaffolds for tissue engineering. *Ceramics International*, *43*(2), 1657-1668. https://doi.org/10.1016/j.ceramint.2016.06.068

[37] Kumar, J. P., Lakshmi, L., Jyothsna, V., Balaji, D., Saravanan, S., Moorthi, A., & Selvamurugan, N. (2014). Synthesis and characterization of diopside particles and their suitability along with chitosan matrix for bone tissue engineering in vitro and in vivo. *Journal of Biomedical Nanotechnology*, *10*(6), 970-981. https://doi.org/10.1166/jbn.2014.1808

[38] Zhou, X., OuYang, J., Li, L., Liu, Q., Liu, C., Tang, M., Deng, Y., & Lei, T. (2019). In vitro and in vivo anti-corrosion properties and bio-compatibility of 5β-TCP/Mg-3Zn scaffold coated with dopamine-gelatin composite. *Surface and Coatings Technology*, *374*, 152-163. https://doi.org/10.1016/j.surfcoat.2019.05.046

[39] Saravanan, S., Chawla, A., Vairamani, M., Sastry, T., Subramanian, K., & Selvamurugan, N. (2017). Scaffolds containing chitosan, gelatin and graphene oxide for bone tissue regeneration in vitro and in vivo. *International Journal of Biological Macromolecules*, *104*, 1975-1985. https://doi.org/10.1016/j.ijbiomac.2017.01.034

[40] Ghasemi, M., Liang, S., Luu, Q. M., & Kempson, I. (2023). The MTT assay: a method for error minimization and interpretation in measuring cytotoxicity and estimating cell viability. In O. Friedrich & D. F. Gilbert (Eds), *Cell viability assays: Methods and protocols* (pp. 15-33). Springer. https://doi.org/10.1007/978-1-0716-3052-5_2

[41] Purohit, S. D., Bhaskar, R., Singh, H., Yadav, I., Gupta, M. K., & Mishra, N. C. (2019). Development of a nanocomposite scaffold of gelatin–alginate–graphene oxide for bone tissue engineering. *International Journal of Biological Macromolecules*, *133*, 592-602. https://doi.org/10.1016/j.ijbiomac.2019.04.113

[42] Ghorbani, F., Sahranavard, M., & Zamanian, A. (2020). Immobilization of gelatin on the oxygen plasma-modified surface of polycaprolactone scaffolds with tunable pore structure for skin tissue engineering. *Journal of Polymer Research*, *27*(9), 1-12. https://doi.org/10.1007/s10965-020-02263-6

[43] Miao, X., Tan, D. M., Li, J., Xiao, Y., & Crawford, R. (2008). Mechanical and biological properties of hydroxyapatite/tricalcium phosphate scaffolds coated with poly (lactic-co-glycolic acid). *Acta Biomaterialia*, *4*(3), 638-645. https://doi.org/10.1016/j.actbio.2007.10.006

[44] Yoshikawa, H., Myiui, A., (2005). Bone tissue engineering with porous hydroxyapatite ceramics, *Journal of Artificial Organs, 8,* 131-136. https://doi.org/10.1007/s10047-005-0292-1

[45] Gibson, L. J., Ashby, M. F. (1999). Cancellous bone. In *Cellular solids: structure and properties* (2nd ed., pp. 429-452). Cambridge University Press.